



Soft-template self-assembly of hierarchical mesoporous SrCO₃ by low-temperature hydrothermal route and their application as adsorbents for methylene blue and heavy metal ions

Wancheng Zhu ^{a,*}, Zuozhong Liang ^a, Xiaofei Liu ^a, Heng Zhang ^a, Yongjun Zheng ^a, Xianglan Piao ^b, Qiang Zhang ^b

^a Department of Chemical Engineering, Qufu Normal University, Shandong 273165, P. R. China

^b Department of Chemical Engineering, Tsinghua University, Beijing 100084, P. R. China

ARTICLE INFO

Article history:

Received 11 December 2011

Received in revised form 24 February 2012

Accepted 22 April 2012

Available online 1 May 2012

Keywords:

Hydrothermal growth

Strontium carbonate

Adsorption

Self-assembly

Hierarchical nanomaterials

ABSTRACT

Toward the efficient and cost effective synthesis of three-dimensional hierarchical architectures at mild condition and their potential applications in environmental protection, the materials chemistry for green synthesis of strontium carbonate (SrCO₃) superstructures and their application as adsorbents for methylene blue solution and heavy metal ions were explored. Uniform hierarchical mesoporous SrCO₃ microspheres with a narrow diameter distribution were synthesized via a mild hydrothermal treatment (110 °C, 6.0 h) of the slurry derived from the room temperature coprecipitation of SrCl₂ and Na₂CO₃ solution, in the presence of ethylenediaminetetraacetic acid (EDTA). The as-synthesized mesoporous SrCO₃ microspheres had a specific surface area of 56.3 m² g⁻¹ and a narrow pore size distribution concentrating on 2–20 nm, with an average pore diameter of 9.45 nm. The introduction of EDTA in due case with tuned pH value was favorable for the formation of SrCO₃ microspheres, whereas the mild hydrothermal treatment promoted the morphology uniformity of the mesoporous microspheres with narrow diameter distribution. The adsorption evaluation indicated that the present mesoporous SrCO₃ microspheres exhibited excellent adsorption performance for deionized (DI) water containing methylene blue, or heavy metal ions such as Fe³⁺ and Pb²⁺, revealing the as-synthesized uniform hierarchical mesoporous SrCO₃ microspheres as potential adsorbents with wide applications in environmental protection.

© 2012 Elsevier B.V. All rights reserved.

1. Introduction

The increased industrial and agricultural activities have resulted in the generation of toxic pollutants such as inorganic anions, metal ions, synthetic organic chemicals, which have poisonous and toxic effects on ecosystems. Many efforts have been made to find facile routes for these contaminant removals in a sustainable and cost effective way. Currently, adsorption is believed to be a simple and effective technique for water and wastewater treatment [1–3]. The success of the adsorption technique largely depends on the development of an efficient adsorbent [4–7]. Activated carbon, clay minerals, zeolites, biomaterials, and some industrial solid wastes have been widely employed as adsorbents for adsorption of ions and organics in wastewater treatment [1–7].

Exploring adsorbent material with low cost and high absorption capacity is a great challenge for sustainable materials chemistry. To realize this, adsorbent materials with required surface properties and porous

structures were designed and produced. Recently, three-dimensional (3D) hierarchical architectures were highly concerned, in which different low-dimensional nanobuilding blocks such as zero-dimensional (0D) nanoparticles (NPs), one-dimensional (1D) nanotubes, nanowires, nanorods, and two-dimensional (2D) nanoflakes well arranged and self-assembled with two or more levels from the nanometer to the macroscopic scale [8–16]. The hierarchical structures, or superstructures, are expected to play an irreplaceable role in fabricating the next generation of microelectronic and photoelectronic devices for their potential application as both building units and interconnections [17]. The applications of hierarchical mesoporous architectures as adsorbents are not fully investigated.

Herein, we explored the idea that hierarchical mesoporous strontium carbonate (SrCO₃) microspheres were used as adsorbents for methylene blue and heavy metal ions removal. The reason we selected SrCO₃ as the target materials was based on the fact that SrCO₃ had been used as additives in the production of iridescent and specialty glasses, pigments, driers, paints, pyrotechnics, sensors [18], catalysts [19,20], strontium metal and other strontium compounds [21], and also as the constituent of ferrite magnets for small direct current motors and an additive in the manufacture of glass for color television

* Corresponding author. Tel.: +86 537 4456301; fax: +86 537 4456305.

E-mail address: zhuwancheng@tsinghua.org.cn (W. Zhu).

tubes [22]. Recently, various 3D architectures of SrCO₃, such as flower-like [23,24], needle-like [25,26], and branch-like [24] etc. have been reported. For example, flower-like SrCO₃ particles have been synthesized via adding surfactants CTAB and SDBS as chemical additives [27], and hierarchical SrCO₃ architectures originated from room temperature aging method (5 days) based on the conversion of pre-synthesized SrCrO₄ nanowires have also been obtained [28]. In addition, spherical or sphere-like SrCO₃ structures [29–32], and especially the mesoporous SrCO₃ spheres have been derived from room temperature ionic liquid (ILs) [33]. Most recently, Wu and co-workers reported an *in vitro* biomineralization of SrCO₃ complex nanostructures by using glucosan as the modifier in dimethyl formamide–deionized (DI) water mixed solvents, and the as-obtained SrCO₃ complex nanostructures showed excellent methylene blue and Rhodamine B adsorption properties and superhydrophobicity [34]. In the previous work, we reported hierarchical SrCO₃ submicron spheres self-assembled by NPs under hydrothermal conditions (190 °C, 12.0 h) with ethylenediaminetetraacetic acid (EDTA) and MgCl₂ as the additives [35,36]. To provide cost effective and efficient SrCO₃ adsorbents, the hydrothermal temperature should be decreased, and mild condition should be explored to realize energy saving, additives simplification as well as environmental benign. The materials chemistry of hierarchical SrCO₃ architecture formation under mild process should thus be investigated to guide their further mass production.

In this contribution, a facile mild hydrothermal route (110 °C, 6.0 h) to hierarchical mesoporous SrCO₃ microspheres was reported, with strontium chloride hexhydrate (SrCl₂·6H₂O) and anhydrous sodium carbonate (Na₂CO₃) as the starting materials and appropriate amount of EDTA solution as the unique additive. The formation mechanism of the mesoporous SrCO₃ microspheres was proposed, and the applications of the mesoporous microspheres as the novel adsorbents for the DI water containing methylene blue or heavy metal ions (e.g. Fe³⁺ and Pb²⁺) were also explored.

2. Experimental

2.1. Low temperature hydrothermal synthesis of hierarchical mesoporous SrCO₃

All reagents were of analytical grade and used directly without further purification. Hierarchical mesoporous SrCO₃ microspheres were synthesized via a room temperature co-precipitation of SrCl₂ and Na₂CO₃ followed by a facile hydrothermal treatment in the presence of appropriate amount of EDTA disodium salt (abbr. as EDTA hereafter) solution as the additive. In a typical procedure, EDTA solution (0.1 mol L⁻¹, 10 mL) was dropped into SrCl₂ (0.5 mol L⁻¹, 20 mL) under vigorous magnetic stirring at room temperature, leading to a clear solution. Then NH₃·H₂O (25–28%) was added into the previously resultant solution to adjust the pH value from 4 to ca. 10 under continuous magnetic stirring for 5–10 min. Subsequently, Na₂CO₃ solution (0.5 mol L⁻¹, 20 mL) was added dropwise, resulted in a white slurry with a molar ratio of EDTA to SrCl₂ as 1:10. The slurry was kept stirring for another 30 min and then transferred into a Teflon-lined stainless steel autoclave. The autoclave was sealed and heated (5 °C min⁻¹) to 110 °C and kept in an isothermal state for 6.0 h and then cooled down to room temperature naturally. The precipitate was filtered, washed with DI water for 3–5 times, and then dried at 70 °C for 24.0 h. To investigate the effect of EDTA and aging time on the formation of SrCO₃, different amount of EDTA (molar ratio, EDTA:SrCl₂:Na₂CO₃ = 0:1:1–1:1:1) was added after all the Na₂CO₃ solution was dropped into the SrCl₂ solution, and the resultant white slurry aged at room temperature for 24.0–504.0 h was washed and dried directly without any further hydrothermal treatment. For EDTA:SrCl₂:Na₂CO₃ = 1:1:1, the pH value of the mixed solution was adjusted to ca.11 after the introduction of EDTA, since SrCO₃ precipitation was failed to be formed under such a significant acidic environment.

2.2. Adsorption properties of hierarchical mesoporous SrCO₃ microspheres

The as-prepared mesoporous SrCO₃ microspheres were employed as adsorbents for the typical methylene blue and heavy metal ions. For the adsorption of methylene blue, the mesoporous SrCO₃ microspheres (30 mg) were added into the prepared methylene blue solutions (500 or 50 mg L⁻¹, 20 mL) under vigorous magnetic stirring at room temperature, keeping the adsorption time within the range of 10–300 min. After filtration, the filtrate was collected for further qualitative and quantitative analysis. The qualitative analysis was performed by monitoring the color change of the filtrate based on the digital pictures captured at different adsorption durations. The quantitative analysis was determined by measuring the absorbency of the filtrate, with the concentration diluted to one tenth of the original value. Based on the obtained absorbency, the degradation rate of the methylene blue could be calculated according to $R = (A_0 - A_1) \div A_0 \times 100\%$, where A_0 and A_1 stand for the absorbency before and after adsorption, respectively [37]. For the heavy metal ions adsorption, SrCO₃ microspheres (30 mg) were added into the prepared FeCl₃ solution (500 mg L⁻¹, 10 mL) under vigorous magnetic stirring at room temperature, keeping the adsorption time within 10–180 min. After filtration, the filtrate was collected. For the qualitative analysis, the filtrate with different adsorption times was added SCN⁻ as color reagents, while the quantitative analysis on the concentration of the Fe³⁺ solution was carried out via measuring the absorbency after the filtrate having been diluted to one-fiftieth of the original value, using the standard curve method. In contrast, for the adsorption of the Pb(NO₃)₂ solution (350 mg L⁻¹, 20 mL), the pH value of solution was adjusted from 6–7 to 2–3 firstly so as to prevent the hydrolyzation of Pb²⁺.

2.3. Characterization

The crystal phase and structure of the samples were identified by an X-ray powder diffractometer (XRD, D8-Advance, Bruker, Germany) using Cu K_α Radiation ($\lambda = 1.54178 \text{ \AA}$) and a fixed power source (40.0 kV, 40.0 mA). The morphology and microstructure of the samples were examined by a field emission scanning electron microscopy (SEM, JSM7401F, JEOL, Japan) and a high resolution transmission electron microscopy (TEM, JEM-2010, JEOL, Japan). The size distribution of the as-synthesized SrCO₃ superstructures was estimated by direct measuring ca. 100 particles from the SEM images. The thermal decomposition behavior was detected by the thermo-gravimetric analyzer (TGA, Netzsch STA 409C, Germany) carried out in dynamic air with a heating rate of 10.0 °C min⁻¹. The porous structure of the sample was characterized by the N₂ adsorption–desorption isotherms, which were measured at 77 K using a Chemisorption–Physisorption Analyzer (Autosorb-1-C, Quantachrome, USA) after the sample had been outgassed at 300 °C for 60 min. The pore size distribution was evaluated from the N₂ desorption isotherm using the Barrett–Joyner–Halenda (BJH) method, and the specific surface area was calculated from the adsorption branches in the relative pressure range of 0.10–0.31 using multi-point Brunauer–Emmett–Teller (BET) method. The absorbency of the ethylene blue or Fe³⁺ solutions adsorbed by mesoporous SrCO₃ microspheres for some time was measured by a UV–vis spectrophotometer (752 type, Shanghai JINGHUA Instruments, China), whereas the concentration of the Pb²⁺ was determined by an inductively coupled plasma-optical emission spectroscopy (ICP-OES, Optima 4300 DV, PerkinElmer, USA) instead of the UV–vis spectrophotometer since no color change was observed during the adsorption of the Pb(NO₃)₂ solution.

3. Results and discussion

3.1. Composition and morphology of the SrCO₃ submicron spheres

Fig. 1 shows the XRD pattern (Fig. 1(a)), SEM (Fig. 1(b, c)), and TEM images (Fig. 1(d)) of the SrCO₃ microspheres hydrothermally

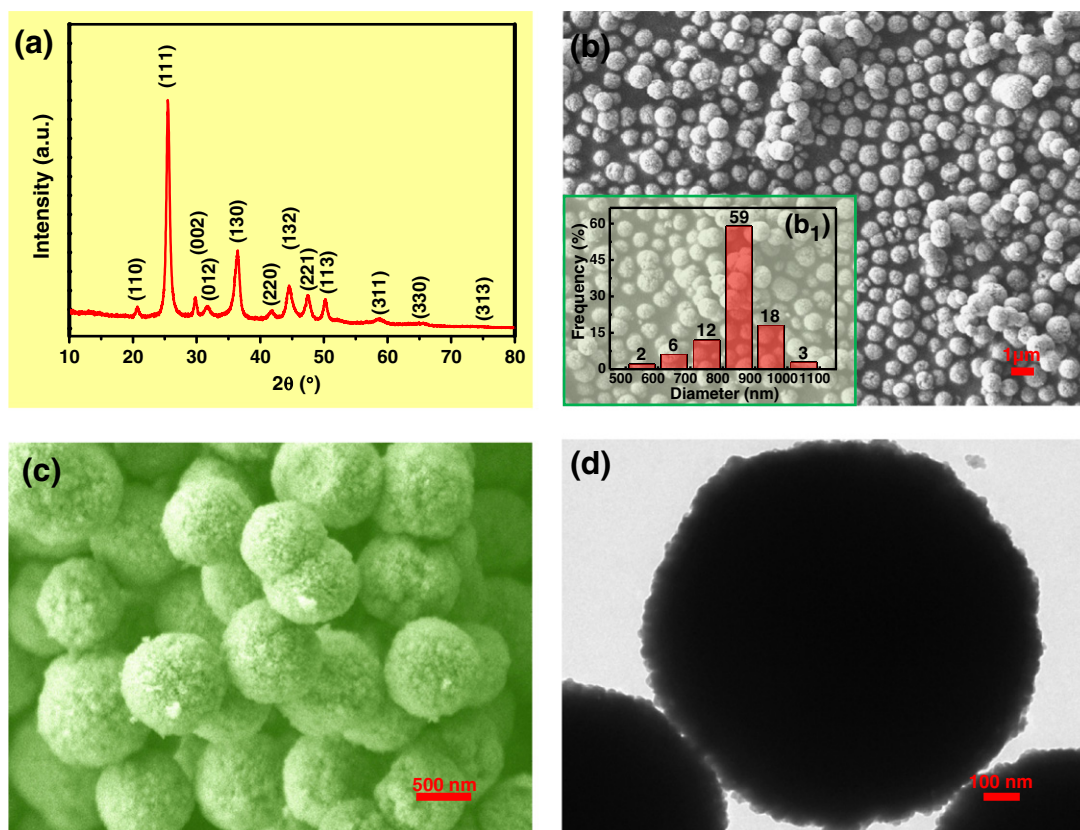


Fig. 1. XRD pattern (a), SEM (b, c) and TEM (d) images of the hydrothermally synthesized porous SrCO₃ microspheres at 110 °C for 6.0 h, in the presence of EDTA (molar ratio, EDTA: SrCl₂:Na₂CO₃ = 0.1:1:1). Inserted figure (b₁) shows the corresponding size distribution of the microspheres.

synthesized at 110 °C for 6.0 h, in the presence of EDTA. All diffraction peaks of the XRD pattern were readily indexed to the orthorhombic SrCO₃ phase (strontianite, PDF No. 05-0418), and no other impurity

peak was detected, indicating the pure phase of the product. The broadening of the diffraction peaks revealed the existence of crystalline SrCO₃ NPs within the structure, and the crystallite size along the [111] direction ($d_{(111)}$) was calculated by the Debye–Scherrer equation as 13.1 nm, smaller than that (14.5 nm) calculated for the crystallite contained in the previously reported SrCO₃ submicron spheres synthesized at 190 °C [36]. The SEM image showed that hierarchical SrCO₃ microspheres with relatively uniform morphology (Fig. 1(b)) and narrow size distribution (Fig. 1(b₁)) were obtained, ca. 90% of which were with a diameter within the range of 700–900 nm (average diameter: 844 nm). Compared with the spherical SrCO₃ particles assisted by EDTA in the ethanol–water mixtures at room temperature [32], mesoporous SrCO₃ microspheres obtained in room temperature ILs [33] and our previously synthesized SrCO₃ microspheres [35,36], the present microspheres demonstrated a significant narrower size distribution. High magnification SEM image (Fig. 1(c)) clearly showed that, the as-synthesized SrCO₃ microspheres consisted of a multitude of tiny NPs (diameter: 10–30 nm) within the body and distinct cavities on the surfaces, in accordance with the broadened XRD pattern (Fig. 1(a)). The TEM image (Fig. 1(d)) reconfirmed the hierarchical superstructures with well defined spherical morphology and constitutional tiny NPs, in agreement with the SEM characterizations.

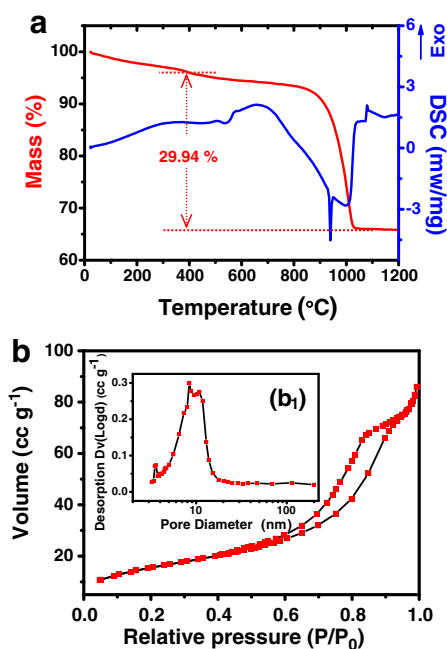


Fig. 2. TG–DSC curves (a) and nitrogen adsorption–desorption isotherms (b) of the porous SrCO₃ microspheres hydrothermally synthesized at 110 °C for 6.0 h, in the presence of EDTA (molar ratio, EDTA: SrCl₂:Na₂CO₃ = 0.1:1:1). Inserted figure (b₁) displays the pore size distribution of the as-prepared porous SrCO₃ microspheres.

3.2. Thermal decomposition and textural properties of the SrCO₃ submicron spheres

Thermal decomposition behavior of the SrCO₃ microspheres was evaluated by the TG–DSC curves, as shown in Fig. 2(a). The mass of the samples decreased gradually from 99.67% (30 °C) to 97.78% (200 °C), 96.04% (396 °C), 93.96% (719 °C), then dropped rapidly to 66.1% (1044 °C), and finally kept relatively constant thereafter. The mass loss of 3.96% before 396 °C was mainly attributed to the elimination of the adsorbed water,

and the subsequent mass loss of 29.94% between 396 and 1044 °C was ascribed to the thermal decomposition of SrCO₃: SrCO₃ (s) → SrO (s) + CO₂ (g). This was similar to the theoretical value for the mass loss of the above decomposition (29.81%), also analogous to those during the thermal decomposition of the SrCO₃ submicron spheres between 400 and 1100 °C [36] and high pure phase SrCO₃ between 900 and 1150 °C. Compared with the SrCO₃ submicron spheres [36], the present SrCO₃ microspheres exhibited relatively lower thermal decomposition temperature, owing to the smaller constitutional crystallites within the microspheres. On the other hand, the simultaneously recorded DSC curve exhibited a small broad endothermic peak and a wide broad endothermic vale within the temperature range of 396–719 °C and 719–1044 °C, corresponded with the gradual dehydration of the adsorbed water and distinct thermal decomposition of SrCO₃, respectively. The significant keen-edged endothermic peak at 920–960 °C was owing to the phase conversion from the orthorhombic α-SrCO₃ to the trigonal β-SrCO₃, in accordance with our previously reported SrCO₃ submicron spheres [36]. It was notable that however, there emerged a remarkable exothermal peak within 1060–1150 °C, which was assumed to be related to the rearrangement

of SrCO₃, similar to some metal borates [38]. For instance, an obvious exothermic peak was also presented on the differential thermal analysis curve of SrB₂O₄ nanorods at high temperature [39].

As shown in Fig. 2(b), the nitrogen adsorption–desorption isotherms of the hydrothermally synthesized SrCO₃ microspheres revealed type IV with an H3-type hysteresis loop at a high relative pressure. This indicated the as-prepared uniform SrCO₃ microspheres of mesoporous structure bearing dominant slit pores and channels of uniform shape and size. Moreover, the corresponding BJH desorption pore size distribution curve (Fig. 2(b₁)) showed that the hierarchical mesoporous SrCO₃ microspheres had a narrow pore size distribution, concentrating on 2–20 nm with an average pore diameter of 9.45 nm, which is larger than that of the mesoporous SrCO₃ spheres obtained in room temperature ILs (5.7 nm) [33] whereas much smaller than that of the mesoporous SrCO₃ submicron spheres (14.4 nm) [35]. The porous structure characterization results demonstrated that the mesoporous SrCO₃ microspheres exhibited a specific surface area of 56.3 m² g⁻¹ and a total pore volume of 0.133 cm³ g⁻¹. The specific surface area of the present microspheres was lower than that of the

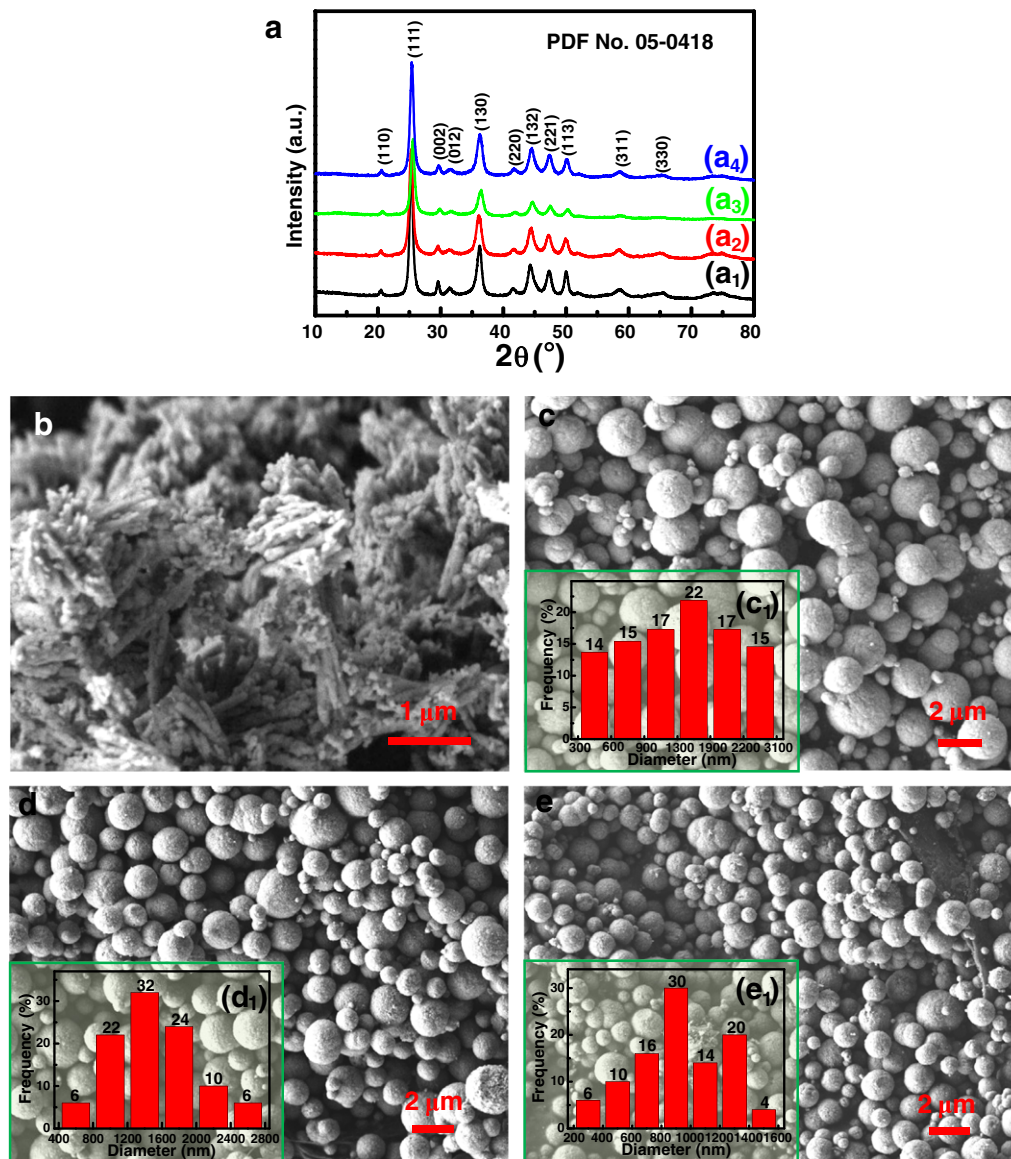


Fig. 3. XRD patterns (a), and SEM images (b–e) of the SrCO₃ particles synthesized in the absence (a₁, b) and presence (a₂–a₄, c–e) of EDTA at room temperature for different time (molar ratio, EDTA:SrCl₂:Na₂CO₃ = 0.1:1:1). Time (h): b–0, c–0, d–12.0, e–84.0. Inset figures (c₁–e₁) show the diameter distributions of the corresponding SrCO₃ microspheres (c–e).

mesoporous SrCO_3 spheres acquired in room temperature ILS ($69.4 \text{ m}^2 \text{ g}^{-1}$) [33] whereas much larger than the hierarchical microsphere complex nanostructures ($10.35 \text{ cm}^2 \text{ g}^{-1}$) [34] and even larger than that of the mesoporous SrCO_3 submicron spheres ($40.2 \text{ m}^2 \text{ g}^{-1}$) [35], due to the relatively smaller constitutional crystallites within the body and also smaller diameter of the present mesoporous microspheres with narrower size distribution.

3.3. Effect of EDTA on the mesoporous SrCO_3 microspheres formation

To illustrate the crucial role of EDTA on the formation of the as-synthesized mesoporous SrCO_3 microspheres, a series of control experiments was performed at room temperature instead of hydrothermal treatment, as shown in Fig. 3. The XRD patterns (Fig. 3(a)) indicated that all the products were of pure phase of strontianite SrCO_3 (PDF No. 05-0418), no matter whether EDTA was present or not in the synthesis process. However, 1D aggregates of SrCO_3 were obtained in the absence of EDTA (Fig. 3(b)). The presence of EDTA promoted the formation of spherical SrCO_3 particles (Fig. 3(c–e)), undoubtedly confirming the crucial role of EDTA on the formation of the present mesoporous SrCO_3 microspheres. Meanwhile, with the aging time prolonging from 0 to 12.0 to 84.0 h, the crystallinity of the as-obtained SrCO_3 spheres became higher to some extent (Fig. 3(a₂–a₄)), the diameter distribution of the microspheres tended to be narrower, and the average diameter also became smaller. When filtered directly without aging, spherical SrCO_3 particles (Fig. 3(c, c₁)) had been available, nevertheless with a wide diameter distribution within the range of 300–3100 nm (average diameter: 1400 nm). With aging time further extending from 12.0 (Fig. 3(d, d₁)) to 84.0 (Fig. 3(e, e₁)) h, the as-obtained SrCO_3 microspheres exhibited a narrower diameter distribution from 400–2800 nm to 200–1600 nm and a smaller average diameter from 1300 nm to 940 nm. Thus, the existence of EDTA was apparently necessary for the formation of spherical SrCO_3 structures; long time aging at room temperature was favorable for the improvement of the uniform morphology and narrow size distribution, whereas the hydrothermal treatment could further enhance such improvement within a short time and ultimately lead to uniform mesoporous SrCO_3 microspheres.

To further investigate the effect of EDTA and aging time on the formation of the SrCO_3 microspheres, extended experiments were carried out. As shown in Fig. S1, when EDTA (molar ratio, EDTA: SrCl_2 : Na_2CO_3 = 0.15:1:1) was added after all the Na_2CO_3 solution was dropped into the SrCl_2 solution, the room temperature precipitates

aged from 24.0 to 168.0 to 336.0 to 504.0 h were all composed of irregular assemblies of SrCO_3 particles. On the other hand, when the aging time was fixed as 168.0 h, no significant changes were observed for the products derived from room temperature precipitation in the presence of more amount of EDTA such as EDTA: SrCl_2 : Na_2CO_3 = 0.4:1:1 (Fig. S2(a, b)), 0.8:1:1 (Fig. S2(a₂, c)). However, with the molar ratio of EDTA: SrCl_2 : Na_2CO_3 further increased to 1:1:1 (Fig. S2(a₃, d)), the product turned to be SrCO_3 microspheres with extremely wide diameter distribution. This indicated that, the additive EDTA was not preferred to be introduced after the addition of Na_2CO_3 solution to acquire uniform SrCO_3 microspheres.

The hydrothermal (Figs. 1 and 2) and room temperature control experimental (Figs. 3, S1 and S2) results showed that, no dumbbell or peanut like intermediate structures were observed throughout the growth of the present SrCO_3 microspheres when the hydrothermal temperature decreased to 110 °C. This is quite different with our previously reported mesoporous SrCO_3 submicron spheres obtained by “rod-to-dumbbell-to-sphere” self-assembly with half amount of EDTA as presently used and MgCl_2 as additives during the 190 °C hydrothermal synthesis [35]. Furthermore, the EDTA was added into the SrCl_2 solution directly, not into the mixture of SrCl_2 and Na_2CO_3 solution. Thus, the EDTA was assumed to be soft template for SrCO_3 nucleation.

3.4. Mechanism of EDTA assisted mesoporous SrCO_3 microspheres formation

As a chelating and capping agent, EDTA has four carboxylic groups and two lone pairs of electrons on two nitrogen atoms as binding sites [40]. Thus as shown in Fig. 4, when the pH value was adjusted to 10 or 11, the introduction of EDTA solution into the initial SrCl_2 solution could lead to relatively stable coordinate compounds of Sr^{2+} -EDTA [41] (Fig. 4(a)) with a relatively large conditional stability constant ($\lg K = 8.73$) under ambient conditions [32]. Then the dropping of CO_3^{2-} into the above clear solution resulted in the nucleation of SrCO_3 owing to the extremely low solubility product ($\lg K_{\text{sp}} = 9.96$), when the degree of supersaturation of the solution reached a certain level. The resultant primary amorphous SrCO_3 nanocrystals (NCs) grew into subcrystals or NPs with longer growth time, with EDTA preferentially adsorbed on the surfaces. On one hand, the coordinate compounds Sr^{2+} -EDTA restrained the rapid release of Sr^{2+} and further inhibited the crystal growth rate, leading to the effective separation of nucleation and growth steps and thus facilitating high-quality

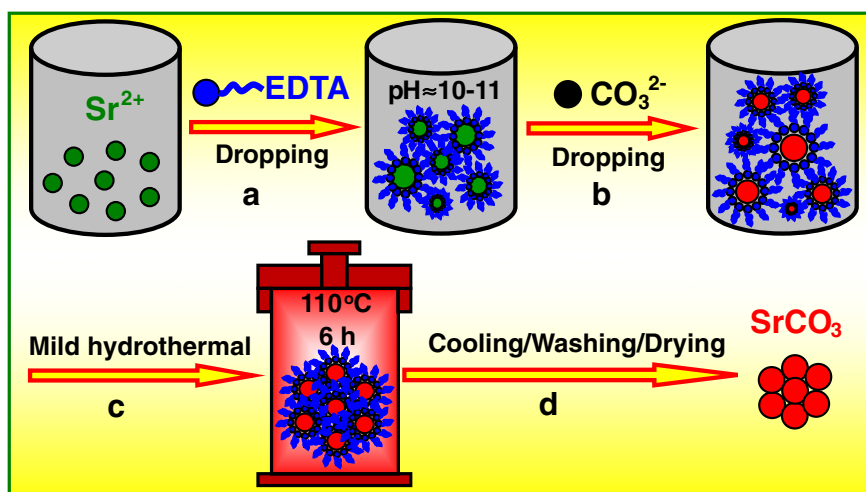


Fig. 4. Schematic illustration of the EDTA soft template assisted self-assembly of hierarchical mesoporous SrCO_3 microspheres. (a) Dropping of EDTA solution into the initial SrCl_2 solution led to formation of the organized coordinate compounds of Sr^{2+} -EDTA after the pH value regulation. (b) Dropping of CO_3^{2-} into the above clear solution resulted in the nucleation and aggregation of SrCO_3 microspheres with broad size distribution. (c) Mild hydrothermal treatment of the previous system at 110 °C for 6.0 h gave rise to uniform SrCO_3 microspheres. (d) Elimination of EDTA via cooling, washing and drying, produced final mesoporous SrCO_3 microspheres.

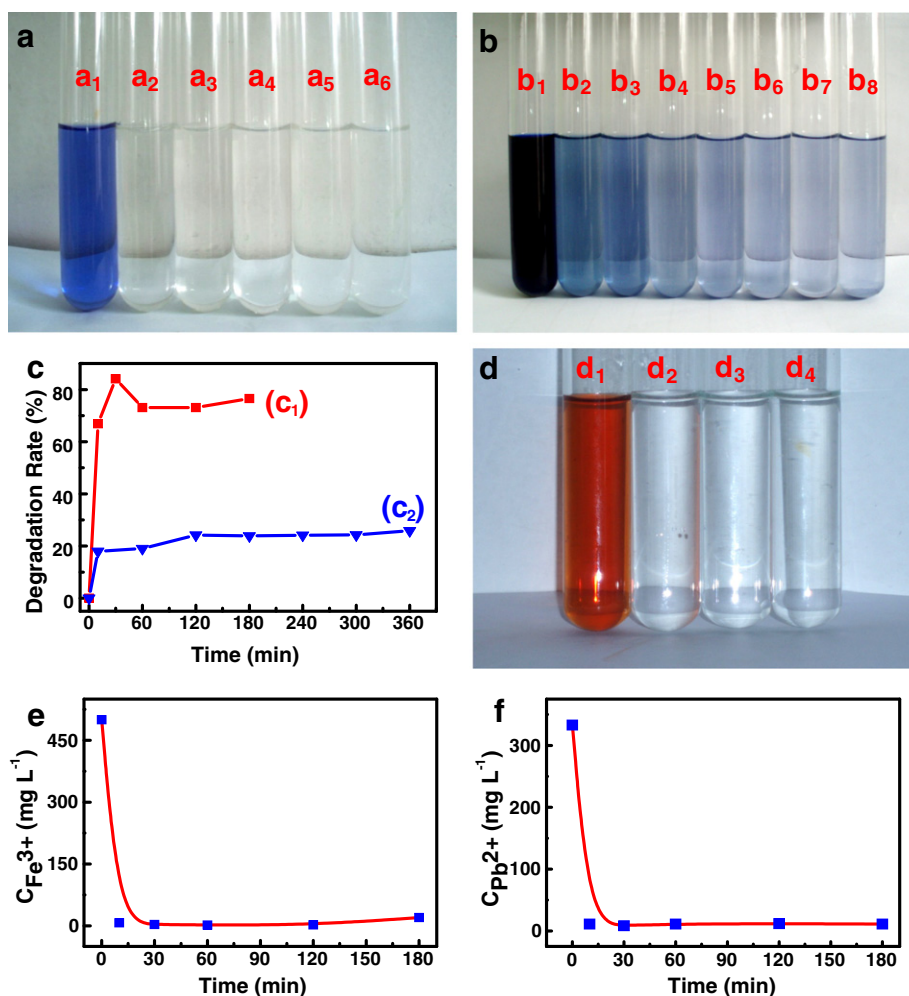


Fig. 5. Mesoporous SrCO₃ microspheres as the adsorbents for methylene blue (a–c) and heavy metal ions (d, e–Fe³⁺; f–Pb²⁺) processed for different durations. Qualitative effects monitored by color change of the solution containing methylene blue (a, b) and heavy metals (d), and quantitative analyses of the variation of the degradation rate (c) or residual concentration of the heavy metal ions (e, f). Concentration of methylene blue (mg L⁻¹): a, c₁–50; b, c₂–500. Concentration of Fe³⁺ or Pb²⁺ (mg L⁻¹): d, e–500; f–350. Adsorption time (min): a₁–0, a₂–10, a₃–30, a₄–60, a₅–120, a₆–180; b₁–0, b₂–10, b₃–60, b₄–120, b₅–180, b₆–240, b₇–300, b₈–360; d₁–0, d₂–60, d₃–120, d₄–180.

crystal synthesis. On the other hand, the carboxyl groups of EDTA afford firm spatial symmetrical configuration, limiting the Sr²⁺ ions within the symmetrical regions. Thus, by using EDTA as modifiers, spherical SrCO₃ particles are facily obtained through the selective absorption of EDTA on the surfaces [41]. In other words, the SrCO₃ NPs with EDTA adsorbed on the surfaces could further aggregate each other, leading to SrCO₃ microspheres, which however were still with broad diameter distribution (Fig. 4(b)). Subsequently, the mild hydrothermal treatment at 110 °C enhanced the Ostwald ripening growth of the tiny SrCO₃ NPs within the as-obtained SrCO₃ microspheres, giving rise to uniform SrCO₃ microspheres within narrow diameter distribution. The further elimination of EDTA via cooling, washing, and drying produced the ultimate hierarchical mesoporous SrCO₃ microspheres, with uniform morphology and narrow diameter distribution.

It was worth noting that, the driving force for Sr²⁺–EDTA formation, the adsorption of EDTA on the surfaces of SrCO₃ NPs, and the aggregation of SrCO₃ NPs with surface-capped by EDTA into hierarchical architectures was believed to be the electrostatic interaction and van der Waals forces, similar to the biomimetic assembly of hierarchical spherical CaCO₃ [42,43], BaCO₃ [44], PbWO₄/CaWO₄ [45], and dumbbell-like SrSO₄ [46]. Moreover, in addition to the irreplaceable effect of EDTA, the pH value also played an important role in the formation of the

present uniform mesoporous SrCO₃ microspheres during the soft template self-assembly process, as confirmed by the control experimental results (Figs. S1 and S2). On the one hand, an appropriate alkaline environment with pH value as 10–11 was favorable for the nucleation and stable existence of SrCO₃ phase. On the other hand, this could promote the dissociation of EDTA and formation of Sr²⁺–EDTA. In contrast with our previous SrCO₃ submicron spheres hydrothermally synthesized at 190 °C for 12.0 h in the presence of bicomponent additives MgCl₂ and EDTA [35], the soft template self-assembly process, instead of “rod-to-dumbbell-to-sphere” growth, provided an alternative milder and easier hydrothermal route to the hierarchical uniform mesoporous SrCO₃ microspheres.

3.5. Application of mesoporous SrCO₃ microspheres as adsorbents

Nowadays, environmental challenges have increasingly gained worldwide concern. The as-synthesized uniform mesoporous SrCO₃ microspheres were employed as adsorbents for methylene blue as well as heavy metal ions, such as Fe³⁺ and Pb²⁺, as shown in Fig. 5. For DI water containing methylene blue with a concentration of 50 mg L⁻¹, the SrCO₃ microspheres exhibited a high adsorption efficiency, confirmed by the significant qualitative color change (Fig. 5(a)) and quantitative degradation rate (Fig. 5(c₁)), which rapidly increased to 66.6%

within 10 min, 84.5% within 30 min, and then vibrated around 73.3%. In contrast, when DI water bearing methylene blue with a much higher concentration as 500 mg L^{-1} was examined, the degradation rate increased to 18.2% within 10 min, however, kept relative stable centered on 24.2% thereafter even though the adsorption time was prolonged to 300 min, confirmed by the gradual color change (Fig. 5(b)) and degradation rate curve (Fig. 5(c₂)). The adsorption efficiency of the present mesoporous SrCO₃ microspheres for methylene blue was much higher than the commercial SrCO₃ powder and also better than that of the SrCO₃ hierarchical microsphere complex nanostructures and rod structures [34] on the whole.

For DI water containing Fe³⁺ (Fig. 5(d, e)) or Pb²⁺ (Fig. 5(f)) ions, the concentration of Fe³⁺ and Pb²⁺ decreased from 500 mg L^{-1} to 4 mg L^{-1} , 350 mg L^{-1} to 10 mg L^{-1} within 10 min, respectively. The final concentration of Fe³⁺ or Pb²⁺ was remained at a low level, as ca. 4 mg L^{-1} and 10 mg L^{-1} , respectively. The adsorption amount of Pb²⁺ by the present mesoporous SrCO₃ microspheres could be estimated as 1.13 mmol g^{-1} , a little lower than that of the mesoporous thiol-functionalized hybrid materials (1.60 mmol g^{-1}) [47]. However, the overall adsorption efficiency of the present mesoporous SrCO₃ microspheres for Fe³⁺ and Pb²⁺ was much higher than that of the zinc silicate nanostructures, including hollow spheres, nanowires, and also membranes [48]. The adsorption results indicated that the present as-synthesized hierarchical uniform mesoporous SrCO₃ microspheres could be employed as ideal adsorbents for water purification, especially for those containing heavy metal ions as Fe³⁺ and Pb²⁺.

4. Conclusions

Uniform hierarchical mesoporous SrCO₃ microspheres were synthesized via a mild hydrothermal treatment (110 °C, 6.0 h) of the slurry derived from the room temperature coprecipitation of SrCl₂ and Na₂CO₃ solution, in the presence of appropriate amount of EDTA as the soft templates. The as-obtained mesoporous SrCO₃ microspheres exhibited a narrow diameter distribution, ca. 90% of which were within 700–900 nm. The SrCO₃ microspheres decomposed within 396–1044 °C, accompanied by a small broad endothermic peak (396–719 °C) and a wide broad endothermic vale (719–1044 °C) containing a significant keen-edged endothermic peak (920–960 °C) on the DSC curve. The N₂ adsorption-desorption isotherms and multi-point BET results confirmed the uniform SrCO₃ microspheres of mesoporous structure with a specific surface area of $56.3 \text{ m}^2 \text{ g}^{-1}$ and a narrow pore size distribution concentrating on 2–20 nm with an average pore diameter of 9.45 nm. A soft-template self-assembly formation mechanism was proposed, based on the control experimental results. Introducing appropriate amount of EDTA with pH value tuned to 10–11 before the dropwise addition of Na₂CO₃ was favorable for the formation of SrCO₃ microspheres, whereas the mild hydrothermal treatment promoted the Ostwald ripening growth of the tiny SrCO₃ NPs within the SrCO₃ microspheres, leading to uniform hierarchical mesoporous microspheres with narrow diameter distribution after the elimination of EDTA. Moreover, the as-prepared mesoporous SrCO₃ microspheres demonstrated excellent adsorption performance for DI water containing methylene blue, or heavy metal ions such as Fe³⁺ and Pb²⁺, indicating the present uniform hierarchical mesoporous SrCO₃ microspheres as ideal potential adsorbents platform, which might also be expected for the adsorption or removal of other dyes or heavy metal ions in water treatment.

Acknowledgments

This work was supported by the State Key Laboratory of Chemical Engineering, China (No. SKL-ChE-09A02), the Project of Shandong Province Higher Educational Science and Technology Program, China (J10LB15), the Excellent Middle-Aged and Young Scientist Award Foundation of Shandong Province, China (BS2010CL024), and the China Postdoctoral Science Foundation (2011M500022).

Appendix A. Supplementary data

XRD patterns and SEM images of the SrCO₃ particles synthesized at room temperature for different aging times, with different amount of EDTA added after the accomplishment of dropping the Na₂CO₃ solution into the SrCl₂ solution are provided and are available online. Supplementary data to this article can be found online at <http://dx.doi.org/10.1016/j.powtec.2012.04.038>.

References

- [1] F.R. Ahmad, A. Pendashteh, L.C. Abdullah, D.R.A. Biak, S.S. Madaeni, Z.Z. Abidin, *Journal of Hazardous Materials* 170 (2009) 530–551.
- [2] Z.J. Fan, J. Yan, G.Q. Ning, T. Wei, W.Z. Qian, S.J. Zhang, C. Zheng, Q. Zhang, F. Wei, *Carbon* 48 (2010) 4197–4200.
- [3] S.B. Wang, Y.L. Peng, *Chemical Engineering Journal* 156 (2010) 11–24.
- [4] M.Q. Zhao, J.Q. Huang, Q. Zhang, W.L. Luo, F. Wei, *Applied Clay Science* 53 (2011) 1–7.
- [5] R.Z. Chen, C.Y. Zhi, H. Yang, Y. Bando, Z.Y. Zhang, N. Sugiur, D. Golberg, *Journal of Colloid and Interface Science* 359 (2011) 261–268.
- [6] L. Chen, T.J. Wang, H.X. Wu, Y. Jin, Y. Zhang, X.M. Dou, *Powder Technology* 206 (2011) 291–296.
- [7] H.X. Wu, T.J. Wang, L. Chen, Y. Jin, Y. Zhang, X.M. Dou, *Powder Technology* 209 (2011) 92–97.
- [8] X.X. Xu, X. Wang, A. Nisar, X. Liang, J. Zhuang, S. Hu, Y. Zhuang, *Advanced Materials* 20 (2008) 3702–3708.
- [9] M.Q. Zhao, Q. Zhang, J.Q. Huang, F. Wei, *Advanced Functional Materials* 22 (2012) 675–694.
- [10] Q. Zhang, M.Q. Zhao, Y. Liu, A.Y. Cao, W.Z. Qian, Y.F. Lu, F. Wei, *Advanced Materials* 21 (2009) 2876–2880.
- [11] M.Q. Zhao, Q. Zhang, X.L. Jia, J.Q. Huang, Y.H. Zhang, F. Wei, *Advanced Functional Materials* 20 (2010) 677–685.
- [12] H. Qian, E.S. Greenhalgh, M.S.P. Shaffer, A. Bismarck, *Journal of Materials Chemistry* 20 (2010) 4751–4762.
- [13] J.Q. Hu, Y. Bando, J.H. Zhan, X.L. Yuan, T. Sekiguchi, D. Golberg, *Advanced Materials* 17 (2005) 971–975.
- [14] K. Sun, Y. Jing, N. Park, C. Li, Y. Bando, D.L. Wang, *Journal of the American Chemical Society* 132 (2010) 15465–15467.
- [15] R.T. Lv, T.X. Cui, M.S. Jun, Q. Zhang, A.Y. Cao, D.S. Su, Z.J. Zhang, S.H. Yoon, J. Miyawaki, I. Mochida, F.Y. Kang, *Advanced Functional Materials* 21 (2011) 999–1006.
- [16] W.C. Zhu, X.L. Wang, X. Zhang, H. Zhang, Q. Zhang, *Crystal Growth & Design* 11 (2011) 2935–2941.
- [17] H.J. Fan, P. Werner, M. Zacharias, *Small* 2 (2006) 700–717.
- [18] J. Shi, J. Li, Y. Zhu, F. Wei, X. Zhang, *Analytica Chimica Acta* 466 (2002) 69–78.
- [19] L. Wang, Y. Zhu, *The Journal of Physical Chemistry. B* 109 (2005) 5118–5123.
- [20] K. Omata, Y. Kobayashi, M. Yamada, *Energy & Fuels* 23 (2009) 1931–1935.
- [21] A.F. Zeller, *Chemische Technik* 19 (1981) 762–768.
- [22] T.J. Bastow, *Chemical Physics Letters* 354 (2002) 156–159.
- [23] S. Li, H. Zhang, J. Xu, D. Yang, *Materials Letters* 59 (2005) 420.
- [24] M.G. Ma, Y.J. Zhu, *Materials Letters* 62 (2008) 2512–2515.
- [25] J. Küther, M. Bartz, R. Seshadri, G.B.M. Vaughan, W. Tremel, *Journal of Materials Chemistry* 11 (2001) 503–506.
- [26] D. Rautaray, A. Sanyal, S.D. Adyanthaya, A. Ahmad, M. Sastry, *Langmuir* 20 (2004) 6827–6833.
- [27] M.X. Zhang, J.C. Huo, H.B. Wang, S.X. Liu, Y.L. Lei, C.P. Cui, *Journal of Synthetic Crystals* 36 (2007) 1136–1140.
- [28] W.S. Wang, L. Zhen, C.Y. Xu, L. Yang, W.-Z. Shao, *Crystal Growth & Design* 8 (2008) 1734–1740.
- [29] M.G. Ma, Y.J. Zhu, *Journal of Nanoscience and Nanotechnology* 7 (2007) 4552–4556.
- [30] I. Sondi, E. Matijević, *Chemistry of Materials* 15 (2003) 1322–1326.
- [31] M. Cao, X. Wu, X. He, C. Hu, *Langmuir* 21 (2005) 6093–6096.
- [32] M.X. Zhang, J.C. Huo, Y.S. Yu, C.P. Cui, Y.L. Lei, *Chinese Journal of Structural Chemistry* 27 (2008) 1223–1229.
- [33] J. Du, Z. Liu, B. Han, Y. Huang, J. Zhang, *Microporous and Mesoporous Materials* 83 (2005) 145–149.
- [34] S.S. Wu, S.F. Yin, H.Q. Cao, Y.X. Lu, J.F. Yin, B.J. Li, *Journal of Materials Chemistry* 21 (2011) 8734–8741.
- [35] W.C. Zhu, G.L. Zhang, J. Li, Q. Zhang, X.L. Piao, S.L. Zhu, *CrystEngComm* 12 (2010) 1795–1802.
- [36] W.C. Zhu, G.L. Zhang, C.M. Liu, Q. Zhang, S.L. Zhu, *Crystal Research and Technology* 45 (2010) 845–850.
- [37] S. Han, J.B. Sun, W. Xiang, S.Y. Guo, F.L. Wang, L. Jiang, D.P. He, *Advanced Materials Research* 183–185 (2011) 1803–1806.
- [38] W.C. Zhu, L. Xiang, Q. Zhang, X.Y. Zhang, L. Hu, S.L. Zhu, *Journal of Crystal Growth* 310 (2008) 4262–4267.
- [39] R. Li, L.H. Bao, X.D. Li, *CrystEngComm* 13 (2011) 5858–5862.
- [40] L. Xu, J. Shen, C. Lu, Y. Chen, W. Hou, *Crystal Growth & Design* 9 (2009) 3129–3136.
- [41] M.N. Pace, M.A. Mayes, P.M. Jardine, L.D. McKay, X.L. Yin, T.L. Mehlhorn, Q. Liu, H. Gürleyük, *Journal of Contaminant Hydrology* 91 (2007) 267–287.

- [42] Z.P. Zhang, D.M. Gao, H. Zhao, C.G. Xie, G.J. Guan, D.P. Wang, S.H. Yu, *The Journal of Physical Chemistry. B* 110 (2006) 8613–8618.
- [43] X.H. Guo, A.W. Xu, S.H. Yu, *Crystal Growth & Design* 8 (2008) 1233–1242.
- [44] S.H. Yu, H. Colfen, A.W. Xu, W.F. Dong, *Crystal Growth & Design* 4 (2004) 33–37.
- [45] Q. Zhang, W.T. Yao, X.Y. Chen, L.W. Zhu, Y.B. Fu, G.B. Zhang, L. Sheng, S.H. Yu, *Crystal Growth & Design* 7 (2007) 1423–1431.
- [46] Y.F. Li, J.H. Ouyang, Y. Zhou, X.S. Liang, T. Murakami, S. Sasaki, *Journal of Crystal Growth* 312 (2010) 1886–1890.
- [47] X. Zhuang, Q. Zhao, Y. Wan, *Journal of Materials Chemistry* 20 (2010) 4715–4724.
- [48] Y. Yang, Y. Zhuang, Y. He, B. Bai, X. Wang, *Nano Research* 3 (2010) 581–593.